Loss of Neurogenesis in Aging *Hydra*

Szymon Tomczyk [1,2] Wanda Buzgariu,[1,2] Chrystelle Perruchoud,[1,2] Kathleen Fisher,[3] Steven Austad,[3] Brigitte Galliot [1,2]

[1] Faculty of Sciences, Department of Genetics and Evolution, University of Geneva, Geneva, Switzerland

[2] iGE3 - Institute for Genomics and Genetics in Geneva, Geneva, Switzerland

[3] Department of Biology, University of Alabama at Birmingham, Birmingham, Alabama

Received 16 October 2018; revised 27 February 2019; accepted 14 March 2019

ABSTRACT: In *Hydra* the nervous system is composed of neurons and mechanosensory cells that differentiate from interstitial stem cells (ISCs), which also provide gland cells and germ cells. The adult nervous system is actively maintained through continuous *de novo* neurogenesis that occurs at two distinct paces, slow in intact animals and fast in regenerating ones. Surprisingly *Hydra vulgaris* survive the elimination of cycling interstitial cells and the subsequent loss of neurogenesis if force-fed. By contrast, *H. oligactis* animals exposed to cold temperature undergo gametogenesis and a concomitant progressive loss of neurogenesis. In the cold-sensitive strain *Ho_CS*, this loss irreversibly leads to aging and animal death. Within four weeks, *Ho_CS* animals lose their contractility, feeding response, and reaction to light. Meanwhile, two positive regulators of neurogenesis, the homeoprotein prdl-a and the neuropeptide *Hym-355*, are no longer expressed, while the "old" RFamide-expressing neurons persist. A comparative transcriptomic analysis performed in cold-sensitive and cold-resistant strains confirms the downregulation of classical neuronal markers during aging but also shows the upregulation of putative regulators of neurotransmission and neurogenesis such as *AHR, FGFR, FoxJ3, Fral2, Jagged, Meis1, Notch, Otx1,* and *TCF15*. The switch of *Fral2* expression from neurons to germ cells suggests that in aging animals, the neurogenic program active in ISCs is re-routed to germ cells, preventing *de novo* neurogenesis and impacting animal survival. © 2019 The Authors. Developmental Neurobiology Published by Wiley Periodicals, Inc. 79: 479–496, 2019

***Keywords: Hydra* nervous system; interstitial stem cells; adult *de novo* neurogenesis; gametogenesis; aging; homeoprotein prdl-a; neuropeptide Hym-355; evolution of neurogenesis**

INTRODUCTION

The freshwater hydrozoan *Hydra* polyp (Fig. 1A) belongs to Cnidaria, a phylum that includes anthozoans (sea anemones and corals) and medusozoans (jellyfish) (Collins *et al.*, 2006). Their common ancestor arose prior to the common ancestor of bilaterians (Fig. 1B) and Cnidaria together with Bilateria are eumetazoans, that is, animals equipped with a nervous system and epithelial layers, the internal one forming a gut, and the external one an epidermis (Fig. 1C). Among cnidarians, the hydrozoan *Hydra* polyp is well known for its amazing capacity to regenerate within few days any missing body part after amputation including its complete

Corresponding to: B. Galliot (brigitte.galliot@unige.ch)

Contract grant sponsor: Foundation for the National Institutes of Health; contract grant number: R01AG037962.

Contract grant sponsor: Schweizerischer Nationalfonds zur Förderung der Wissenschaftlichen Forschung; contract grant number: 31003A_149630, 31003_169930.

Contract grant sponsor: Claraz donation and the Canton of Geneva

Contract grant sponsor: Canton of Geneva

Additional Supporting Information may be found in the online version of this article.

Published online 26 April 2019 in Wiley Online Library (wileyonlinelibrary.com).

DOI 10.1002/dneu.22676

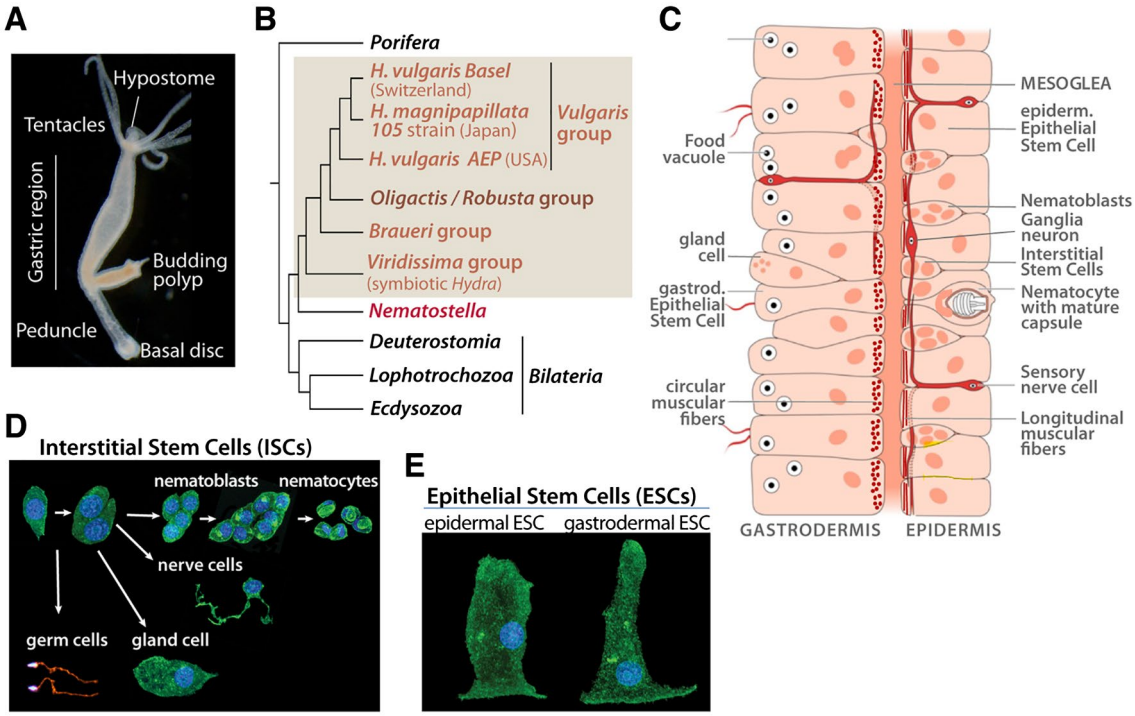

Figure 1 *Hydra* anatomy, phylogenetic position and cell types. (A) Bright field picture of a budding *H. oligactis*. Note the typical stalk shape of the peduncle region. (B) Phylogenetic tree showing the respective positions of *H. vulgaris* and *H. oligactis*. (C) Schematic view of the bilayered organization of the body column with the gastrodermis (or gut) on the left side and the epidermis on the right one, separated by an acellular matrix named mesoglea. Epithelial cells from both layers contain myofibrils, circular in gESCs and longitudinal in eESCs. Nematoblasts and nematocytes are restricted to the epidermis while nerve cells are present in both layers although more abundant in the outer one. Scheme modified from (Lenhoff and Lenhoff, 1988). (D, E) Identification of the various *Hydra* cell types, as observed after tissue maceration followed by b-tubulin immunodetection and DAPI counter staining. Among the derivatives of the multipotent ISCs (D), note the precursors to nematocytes (or cnidocytes) named nematoblasts that divide syncitially before entering differentiation, and the different types of nerve cells: sensory, sensory/motor (bipolar), or ganglion neurons (multipolar). The ESCs (E) are unusual stem cells, that is, self-renewing and differentiated (Buzgariu et al., 2015). [Colour figure can be viewed at wileyonlinelibrary.com]

nervous system. In fact, the central body column of the animal is populated all along its life with multipotent interstitial stem cells (ISCs) that beside germ cells and gland cells produce all cells of the nervous system, as well as epithelial stem cells in the epidermis (eESCs) and the gastrodermis (gESCs) (Buzgariu *et al.*, 2015). ISCs produce neuronal precursors that migrate toward the extremities of the animal where they differentiate to replace cells that die or get sloughed off (Bode *et al.*, 1973; Fujisawa, 1989; Teragawa and Bode, 1995; Technau and Holstein, 1996). As a consequence, the *Hydra* nervous system is much denser at the apical and basal poles. This process that takes several weeks in homeostatic conditions is completed within several days when the animals regenerate its apical or basal extremity (Wenger *et al.*, 2016).

Cnidarian neurons that form neurites but no typical axons, therefore, often named "nerve cells," can be sensory, sensory-motor bipolar, and multipolar also named ganglia neurons (Fig. 1D). These ganglia neurons function as interneurons that form in some species a well visible nerve ring at the base of the tentacles, often recognized as a simple form of cephalization (Koizumi, 2007). Beside nerve cells, a large pool of mechanosensory cells named cnidocytes or nematocytes contribute to the feeding and defense behaviors, as equipped with a cnidocil that, upon stimulation, triggers the discharge of the cnidocyst, a phylum-specific organelle that functions as a weapon full of venom (Tardent, 1995). The two main cell lineages that form the *Hydra* nervous system are quite different at the quantitative level (Bode *et al.*, 1973; David, 1973), the neurons being rather rare (3% of all

cell types) and functional for several weeks while the abundant nematocytes (35%) are "single-usage," replaced once they have discharged their venom capsule.

Cnidarian and bilaterian nervous systems follow the same principles of synaptic conduction and chemical neurotransmission (Anderson and Spencer, 1989; Kass-Simon and Pierobon, 2007), even though cnidarian neurons heavily make use of peptides with peptide-gated ion channels as receptors (Grimmelikhuijzen and Westfall, 1995a; Grunder and Assmann, 2015). The pool of transcription factors involved in bilaterian neurogenesis are largely expressed in cnidarian nervous systems (Grens *et al.*, 1995; Gauchat *et al.*, 1998; 2004; Miljkovic-Licina *et al.*, 2004; 2007; Galliot *et al.*, 2009; Marlow *et al.*, 2009; Galliot and Quiquand, 2011), suggesting a common origin between cnidarian and bilaterian nervous systems. Still, some neuropeptides impact neuronal differentiation, positively in case of Hym-355 (Takahashi *et al.*, 2000).

Another amazing feature of *Hydra* is its ability to survive short antimitotic treatments (hydroxyurea, colchicine) that eliminate the fast cycling ISCs but leave intact the two epithelial stem cell populations (Campbell, 1976; Marcum and Campbell, 1978; Marcum *et al.*, 1980). Upon such treatments, *de novo* neurogenesis is suppressed and animals progressively loose all their nerve cells. In few weeks, the cell lineages that derive from ISCs are depleted making the animal "nerve-free" (Sacks and Davis, 1979). Surprisingly, such nerve-free animals can survive months and years if manually force-fed and their developmental capacities are not impaired, meaning that animals only equipped with two epithelial layers still regenerate and, if heavily fed, bud. A recent transcriptomic analysis showed that these epithelial cells (Fig. 1E) actually upregulate a large number of genes, including genes normally predominantly expressed in ISCs or their derivatives (Wenger *et al.*, 2016). The functional consequences of these genetic modulations have not been explored yet, but this result highlights an epithelial plasticity at the transcriptional level when neurogenesis fails.

Three main studies performed over the past 70 years indicate that *Hv* polyps have an extremely long lifespan or might even escape aging completely (Brien, 1953; Martínez, 1998; Schaible *et al.*, 2015). The dynamic maintenance of the three populations of stem cells is necessary for slow aging and more specifically the stock of ISCs for maintaining a continuous neurogenesis in adult animals. How *Hydra* polyps maintain over long periods of time stocks of adult stem cells without any DNA-damage or cellular alteration is poorly understood. In a distinct species named *H. oligactis* (Fig. 1A), aging rapidly follows the induction of gametogenesis, which is obtained by transferring the animals from room temperature (RT) to 10°C (Brien, 1953). After few weeks, the intense production of gametes leads to the depletion of the somatic populations derived from ISCs, and animals cannot maintain their fitness (Yoshida *et al.*, 2006).

More recently, we characterized two distinct *H. oligactis* strains that exhibit different responses to cold-induced gametogenesis; one that undergoes aging (*Ho_CS)* and another that resists to aging (*Ho_CR)* (Tomczyk *et al.*, 2017). *Ho_CS* animals exhibit the typical aging phenotype reported by Brien (1953) and Yoshida *et al.* (2006), we also noted the disorganization of the apical nervous system (Tomczyk *et al.*, 2015). At the epithelial level, we identified two main differences between aging-sensitive and aging-resistant animals, (i) the inducibility of the autophagy flux that appears deficient in *Ho_CS,* and (ii) the self-renewal of ESCs that progressively and irreversibly decreases in aging animals (Tomczyk *et al.*, 2017). The importance of autophagy for stem cell homeostasis was demonstrated in multiple cell types as recently reviewed by (Boya *et al.*, 2018). Autophagy also plays a key role in the maturation and survival of adult-generated neurons but the mechanisms remain unknown (Xi *et al.*, 2016). With this study our aim was to characterize at the behavioral, cellular and molecular levels the degeneration of the nervous system in aging *H. oligactis.*

MATERIALS AND METHODS

Hydra Culture and Induction of Aging

Strains of *Hydra vulgaris* (*Hv_Basel)* or *Hydra oligactis,* identified as Cold Sensitive (*Ho_CS*) and Cold Resistant (*Ho_CR)* were mass-cultured in Hydra Medium (HM: 1 mM of NaCl, 1 mM of $CaCl_2$, 0.1 mM of KCl, 0.1 mM of $MgSO_4$, 1 mM of Tris-HCl pH 7.6) and fed twice a week with freshly hatched brine shrimps. To induce aging *Ho_CS* and *Ho_CR* animals were transferred from 18°C ± 0.5°C, the standard temperature for *Hydra* culture, to incubators at 10°C ± 0.3°C. For animals maintained at 10°C all washes were done with pre-cooled HM (10°C) and transferred to sterile cold culture dishes. For transcriptomic analyses, animals from the *Hv_Jussy, Hv_sf1,* and *Hv_AEP* strains were used as reported in Wenger *et al.* (2016).

Behavioral and Morphometric Analyses

For touch responsiveness, animals were stimulated with tweezers in the peduncle region and observed under the binocular and the time between tweezer stimulation and contraction was noted for each

Ho_CS animal maintained either at 18°C or at 10°C for 35 days. For light response, 15 polyps maintained at 18°C or 10°C in dim light were allowed to fully extend in a darkened room, then exposed to a LED light source placed 19 cm above the animals to record body column contractions (at least 25% of their length). The latency period corresponds to the time between initial light exposure and the observed first contraction (5 min at most). For prey capture, 15 polyps per condition were placed in a 24-well plate pre-filled with 1 ml HM containing *Artemia*. After 15 s the animals were transferred to HM-containing wells, the number of captured *Artemia* was recorded and normalized by tentacle number. The variations in hypostome size were measured by manually delimiting the hypostome area on the images taken with Leica DM5500. The delimited surface was measured with Fiji.

Immunofluorescence (IF) on Macerated Tissues and on Whole Mounts

Procedures were as described in (Wenger *et al.*, 2016). Briefly, for IF on cells *Hydra,* tissues were macerated according to (David, 1973). The cell suspension was spread on positively charged Superfrost Plus slides (Thermo Scientific) and dried for two days at RT, then washed in PBS, blocked with PBS, 2% BSA, 0.1% Triton-X100 for 2 h, and incubated with the *anti a-tubulin* antibody overnight at 4°C. After washes in PBSTw (PBS, 0.1% Tween-20), cells were incubated in the anti-rabbit AlexaFluor-488 antibody (1:600, Thermofisher), counterstained with DAPI and imaged on a Leica SP8 confocal microscope. For IF on whole mounts, animals were briefly relaxed in urethane 2% (60 s), then fixed in 4% paraformaldehyde (PFA) prepared in HM when immunodetected with the rabbit polyclonal serum raised against the *RFamide* neuropeptide (Grimmelikhuijzen, 1985; Wenger *et al.*, 2016). When immunodetected with the rabbit polyclonal serum raised against the *prdl-a* homeoprotein (Gauchat *et al.*, 1998), animals were fixed in Lavdowsky fixative (50% of ethanol, 3.7% of formaldehyde, and 4% of acetic acid) for 1 h at 37°C, washed several times in PBS, and incubated in 2N HCl for 30 min for DNA denaturation. Then, whatever the fixation condition, animals were washed in PBS, blocked in PBS, 2% BSA, 0.1% Triton-X100 for 2 h, incubated overnight at 4°C with the primary antibody (1:1,000), washed in PBSTw and incubated with the appropriate anti-rabbit AlexaFluor antibody (AlexaFluor-488 or AlexaFluor-555, 1:600, Thermofisher). The samples were finally washed in PBSTw, DAPI stained and pictured on a Leica SP8 or Zeiss LSM700 confocal microscope.

BrdU Detection and Whole Mount in situ Hybridization (WM-ISH)

Animals were incubated in 5 mM *5′-bromodeoxyuridine (BrdU)* for 4 h, washed and maintained in HM for two days, and fixed in 4% PFA/HM for 4 h then in ethanol overnight at −20°C. The transcripts were detected with a digoxygenin (DIG)-labeled riboprobes specific to *Hym355, prdl-a, TCF15* or *Fral2* and the samples were processed for WM-ISH as in (Bode *et al.*, 2008). In case of *H. oligactis* animals, the WM-ISH procedure was shortened at several steps to account for their higher frailty: proteinase K digestion was 8 and 10 min for animals maintained at 10 and 18°C respectively, the 80°C preheat step was 20 min, the probe hybridization step 16 h and the post-hybridization MAB washes 6 × 15 min. Whatever the species, the hybridized riboprobes were similarly detected by NBT-BCIP staining, the samples were then post-fixed in 3.7% FA for 30 min, washed for 15 min in methanol and 3 × 10 min in PBSTr (PBS, 0.1% Triton X-100). Next, the samples were treated with 2N HCl for 30 min, washed in PBST several times over 15 min, incubated overnight at 4°C with the *anti-BrdU* antibody (1:20, Roche), washed 4 × 10 min in PBS and incubated in the anti-mouse Alexa 488-coupled secondary antibody (1:500, Molecular Probes) for 4 h at RT. Then animals were labeled with DAPI for 10 min, washed in PBS (4 × 10 min), 5 min in H2O, mounted in Mowiol and imaged on a Leica D5500 microscope equipped with a color DMC2900 and a monochromatic DFC9000 camera.

BrdU and prdl-a Double Immuno-Labeling

Intact *H. vulgaris* were incubated with 5 mM BrdU for 4 h and either amputated at mid-gastric level and let to regenerate for four days, or washed and maintained intact in HM. At the indicated time, the animals were fixed for 1 h at 37°C in Lavdowsky "minus" (50% ethanol, 3.7% FA), washed several times in PBS, treated with 2N HCl for 30 min and washed again in PBS. After 1 h incubation in 2% BSA, PBS, the samples were incubated overnight with the *anti-BrdU* (1:20, Roche) and *anti-prdl_a* (1:1,000, Gauchat *et al.*, 1998) antibodies, washed 4 × 10 min in PBS, incubated with the anti-mouse Alexa 488 and anti-rabbit Alexa 555 antibodies (1:500, Molecular Probes), washed again 4 × 10 min in PBS, incubated for 10 min in DAPI (1 μg/ml in PBS), washed 2 × 5 min in PBS, briefly in water and mounted in Mowiol. Imaging was performed with a LSM700 Zeiss confocal microscope. For quantification of interstitial cell proliferation in *Ho_CS,* animals were exposed to BrdU for 24 h at indicated time points of the aging process. At the end of the treatment animals were macerated as in (David,

1973) and immunodetected with the anti-BrdU antibody as described above. The BrdU + nuclei were counted manually to establish the BrdU-labeling index.

Transcriptomic Analyses

The quantitative RNA-sequencing analysis (qRNA-seq) performed on *Ho_CS* and *Ho_CR* animals maintained either at 18°C or at 10°C is detailed in (Tomczyk *et al.*, 2017). The qRNA-seq performed either on *Hv_Jussy* animals sliced at five distinct positions along the body axis (Supplementary Figure S1), or on *Hv_sf1* animals exposed to drugs (hydroxyurea, colchicine) or to heat-shock, or on transgenic *Hv_AEP* animals expressing GFP in one or the other stem cell populations is reported in (Wenger *et al.*, 2016). Values that were obtained in biological triplicates for each condition are available in Table S1 from Wenger *et al.* (2016). For heatmap representations, each value corresponds to the average number of reads obtained at indicated time points. Orthologous relationships between *Hv_sf1, Ho_CR* and *Ho_CS* sequences were assigned manually. GraphPad Prism 7 was used to generate the scatterplots of fold change differences between *Ho* and *Hv* RNA-seq values and the regression analysis. Sequences and RNA-seq profiles are publicly available, for *H. vulgaris* at https://Hydratlas.unige.ch, for *Ho_CS* and *Ho_CR* at http://129.194.56.90/blast/.

RESULTS

Sustained *de novo* Neurogenesis in Long Lived *H. vulgaris*

To demonstrate the *de novo* production of neurons in homeostatic and regenerating non-aging animals we used two established markers for neuronal progenitors and nerve cells, the homeoprotein prdl-a and the neuropeptide *Hym-355*, respectively. Both prdl-a and Hym-355 are involved in the control of neurogenesis, prdl-a in the production of apical neuronal progenitors (Gauchat *et al.*, 1998), Hym-355 in the neuronal differentiation of interstitial progenitors (Takahashi *et al.*, 2000). In homeostatic conditions, both *prdl-a* transcripts and the prdl-a protein are predominantly expressed in apical interstitial progenitors (Fig. 2A,D) while *Hym-355* is expressed in apical and basal subpopulations of neurons, and to a lower extent in the body column (Fig. 2A,B). The animals fixed four days after a short exposure to BrdU do not show any BrdU + cells that express *Hym-355* (Fig. 2B). Under homeostatic conditions, the number of neurons produced each day is rather low as *de novo* neurogenesis is slow (Hager and David, 1997), explaining why BrdU/*Hym-355* positive neurons cannot be detected in this condition.

During regeneration, the dense nervous systems in the head and peduncle are re-established, in few days to maintain the animal fitness. Immediately after amputation, neuronal progenitors migrate toward the wound to contribute to the regeneration of the nervous system in the newly formed structure. In the regenerating tips the expression of *prdl-a* and *Hym-355* is re-established with different kinetics: *prdl-a* shows a dual regulation with a first immediate but transient expression in gastrodermal cells (Gauchat *et al.*, 1998), followed by an upregulation in interstitial progenitors of the head-regenerating tip from 16 h post-amputation (hpa) (Fig. 2C). By contrast, *Hym-355* starts to be upregulated later, detected in both the head- and foot-regenerating tips after 24 hpa (Fig. 2C). To visualize the induction of neurogenesis in regenerating animals, we coupled prdl-a immunodetection to BrdU labeling: *H. vulgaris* animals bisected at mid-gastric position were immediately exposed to BrdU for 4 h, then left to regenerate for four days and fixed for immunodetection. In such conditions, we noticed a high increase in the number of $BrdU^+$/prdl-a^+ nuclei when compared to non-bisected animals (Fig. 2D), reflecting the anticipated fast neurogenesis process.

These two types of *de novo* neurogenesis, slow in intact animals and fast in regenerating ones, do not seem to be altered in animals kept for several years as these animals regenerate well the missing structures and maintain their active behaviors, that is, feeding, contracting, and walking (Brien, 1953; Martínez, 1998). By contrast, *H. oligactis* animals exposed to cold temperature, a condition that induces gametogenesis, rapidly loose their fitness and the ability to maintain a dynamic neurogenesis (Brien, 1953; Yoshida *et al.*, 2006; Tomczyk *et al.*, 2015) (Fig. 3A).

Aging *H. oligactis* Lose Their Contractility and Feeding Capacity

To test the impact of aging on the various functions of the nervous system, we compared the behaviors of aging and non-aging animals exposed to mechanical stimulus, light, or food. We first tested the contractility induced by a mechanical stimulus, that is, a pinch in the peduncle region (Fig. 3B). We found that while *Ho_CS* animals maintained at 18°C contract within 2 s, *Ho_CS* animals taken 35 days after transfer to 10°C show a much slower reaction time of 10 s (see supplementary movies). We also measured

at regular time-points over a 30 days period after transfer to 10°C, the contraction latency in response to light (Fig. 3C). We recorded an increase in the contraction latency, from 40 to 100 s in *Ho_CS* animals while the initial value (60 s) remained stable in *Ho_CR* animals exposed to cold for the same period of time (Fig. 3C).

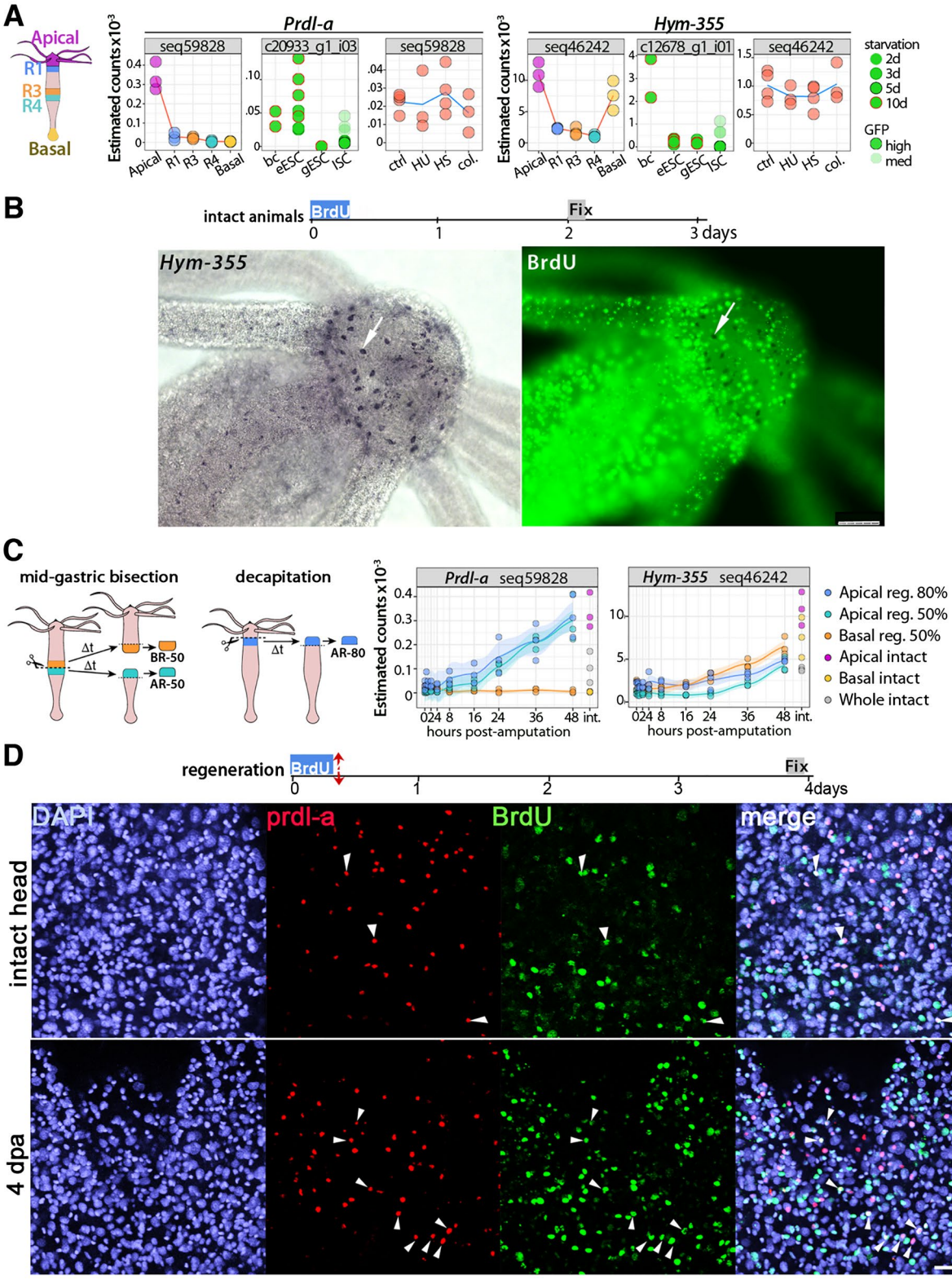

Figure 2 Homeostatic and regeneration-induced *de novo* neurogenesis in slow aging *Hydra vulgaris*. (A) Expression profiles of the neurogenic genes *Prdl-a* and *Hym-355* as detected in animals of the heat-sensitive *Hv_sf-1* strain through three different RNA-seq approaches performed (a) on tissues from slices of the body column when distinct regions (Head, R1, R3, R4, Foot) were dissected before RNA extraction (see the scheme on the left that indicates the five regions); (b) on distinct cell types, that is, ectodermal epithelial stem cells (eESC), gastrodermal epithelial stem cells (gESC), and interstitial stem cells (ISCs) isolated by flow-cytometry; (c) on the central body column of animals exposed to drugs (HU and colchicine) or Heat-shock (HS). All transcriptomic procedures are described in (Wenger et al., 2016). (B) Lack of $BrdU^+$ neurons expressing *Hym-355* in animals exposed to BrdU for 4 h and fixed four days later. Scale bar: 25 μm (left) and 75 μm (right). (C) Expression profiles of *Prdl-a* and *Hym-355* transcripts detected by RNA-seq in regenerating-tips dissected at various time points of head or foot regeneration. Animals were either bisected at mid-gastric level (50%) or decapitated (80%). (D) Prdl-a (red) and BrdU (green) co-detection in the apex of intact (upper panel) or head-regenerating (lower panel) *H. vulgaris* animals. All animals were exposed to a 4 h BrdU pulse, then immediately bisected at mid-gastric level and fixed three days later. In the apical region shown here prdl-a expression is nuclear, enhanced in regenerating heads (Gauchat et al., 1998). The prdl-a^+ and prdl-a^+/$BrdU^+$ cells (white arrowheads) are rare in heads of intact animals but numerous in newly regenerated heads. Scale bar: 25 μm. [Colour figure can be viewed at wileyonlinelibrary.com]

The difference between the two strains was already visible at day-14 after the temperature switch.

The feeding behavior in *Hydra* is characterized by the capture of preys on the tentacles, the subsequent opening of the mouth and the coordinated movement of the tentacles to favor the ingestion of the preys through the mouth. This complex behavior is triggered by reduced glutathione release from the captured prey (Loomis, 1955; Grosvenor *et al.*, 1996; Pierobon, 2015). Here animals were individually exposed to preys, that is, swimming *Artemias*, for 15 s and the number of preys fixed on the tentacles was counted. This test that was performed at various time points after transfer to 10°C, showed a continuous decline in the ability to fix preys in *Ho_CS* animals, already visible at day-14 post-transfer, but not in *Ho_CR* ones (Fig. 3D). After 30 days, a single prey was fixed on average on tentacles of *Ho_CS* animals versus six in *Ho_CR* animals. This decline reflects the inability of the animals to produce functional nematocytes that are normally abundant along the tentacles. After five to six weeks at 10°C, prey capture becomes impossible for *Ho_CS* animals as their head structures are heavily degenerated. These results show that both the contractility in response to light and the capacity to capture preys start to decline within 14 days after transfer to cold in *Ho_CS* but not in *Ho_CR*, progressively decreasing over the following weeks. This indicates that deficiencies in both neurogenesis and nematogenesis precede the morphological changes that appear at day-30.

Degeneration of the Nervous System in Aging *H. oligactis*

To investigate the nervous systems of the animals that show a decline of their behavioral functions, we analyzed the nerve cell density along the animal body, first by monitoring the distribution of the *Hym-355* expressing neurons in *Ho_CS* animals undergoing aging. At 18°C, *Hym-355* neurons distribute in the apical and basal regions as well as along the body column in *Ho_CS* animals (Fig. 4A). In *H. vulgaris Hym-355* was described as predominantly expressed at the extremities, with only a low number of *Hym-355* neurons present in the body column (Takahashi *et al.*, 2000). In *H. oligactis* as in *H. vulgaris, Hym-355* expression is restricted to nerve cells however *Hym-355* neurons are also numerous along the body axis, indicating species-specific variations. After one month at 10°C, we observed a severe loss of *Hym-355* + nerve cells, which are no longer detected after 41 days (Fig. 4A).

In parallel, we detected RFamide expressing neurons in *Ho_CS* and *Ho_CR* animals maintained at 18°C or at 10°C (Fig. 4B). RFamides are neuropeptides widely expressed in mature nerve cells along the body axis and at the extremities, highlighting the higher density of the nervous system at the apex and along the peduncle (Grimmelikhuijzen, 1985). As a low fraction of *Ho_CS* and *Ho_CR* animals do not undergo gametogenesis after transfer to cold, we used sexual and asexual animals maintained for 36 days at 10°C to discriminate between the effects of cold stress versus gametogenesis and aging on the nervous system. We noted an obvious lower density of $RFamide^+$ nerve cells in the upper part of the body column in sexual *Ho_CS* animals, well visible in the region directly below the head. We noted the persistence of "old" $RFamide^+$ neurons at the apical extremity as well as in the peduncle region although the nerve net appears disorganized (Fig. 4B). In contrast, *Ho_CR* animals,

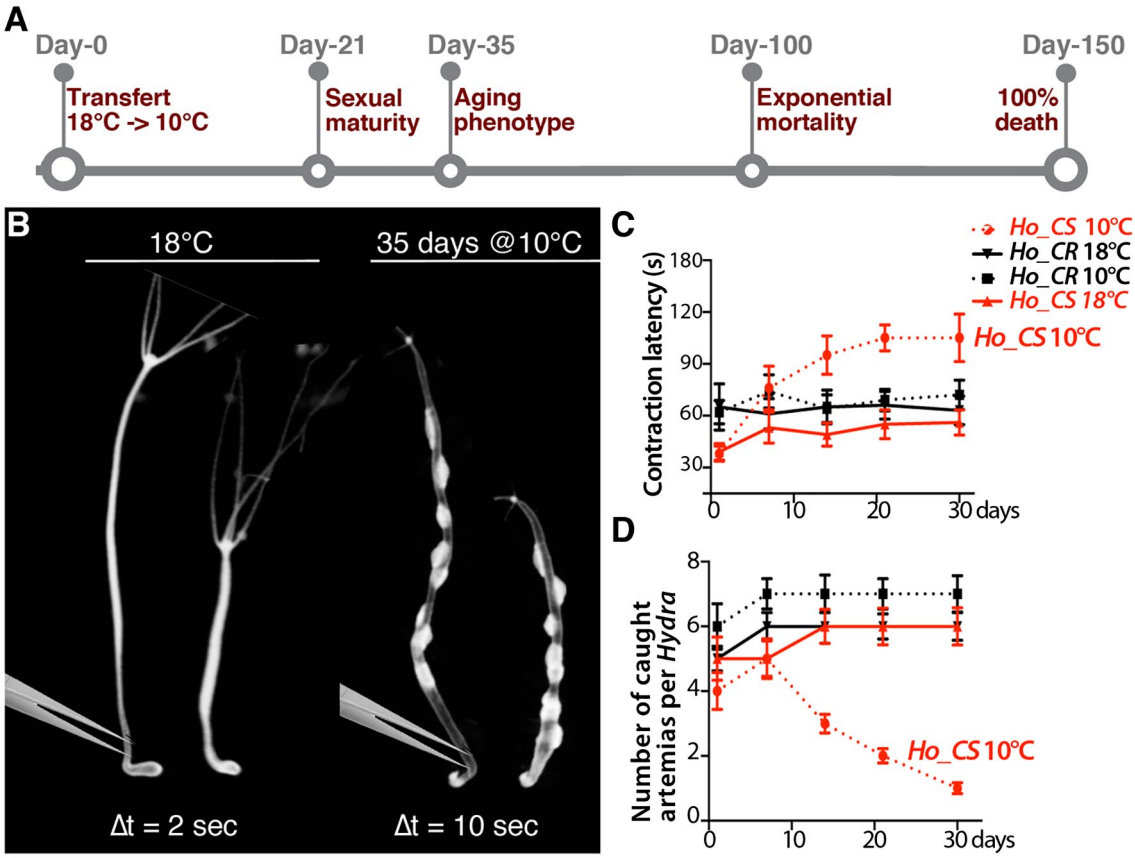

Figure 3 Behavioral alterations in *H. oligactis* animals undergoing aging. (A) Schematic view of the aging process induced in sexual *H. oligactis* cold-sensitive (*Ho_CS*) animals that undergo gametogenesis upon transfer to cold (10°C). Animals from the closely related *H. oligactis* cold-resistant strain (*Ho_CR)* also undergo gametogenesis within three weeks but do not exhibit any aging phenotype and remain fit over the following months (Tomczyk et al., 2017). (B) Contractility upon mechanical stimulation in *Ho_CS* animals maintained either at 18°C or at 10°C for 35 days. The contractility in response to tweezer stimulation of the peduncle region was recorded on live animals imaged with an Olympus SZX10 microscope equipped with a DP73 camera (movie). Contraction of the whole animal body takes place within 2 s in animals maintained at 18°C and within 10 s in *Ho_CS* animals maintained at 10°C for 35 days. (C) Light-induced contractility of *Ho_CS* and *Ho_CR* animals maintained at 10°C (n = 15). The contractility was deduced from the time taken by the animal to elaborate a typical contraction response to a bright, directly focused light source. (D) Prey capture of *Ho_CS* and *Ho_CR* animals maintained at 10°C (n = 15) assessed from the number of *Artemia* fixed on tentacles of each animal normalized by tentacle number. In C and D, the legend codes are the same and the error bars correspond to standard error of the mean (SEM). Note that already two weeks after transfer to 10°C, *Ho_CS* but not *Ho_CR* animals show an extended contraction latency after light exposure and lose the ability to capture preys. [Colour figure can be viewed at wileyonlinelibrary.com]

sexual, or asexual, maintained at 10°C for 36 days exhibit a nervous system that is not modified in terms of density or organization. Both neuronal markers, *Hym-355* and prdl-a, point to a clear degeneration of the nervous system in sexual *Ho_CS* animals maintained for weeks at 10°C.

Loss of *de novo* Neurogenesis in Aging *Hydra Oligactis*

The observed loss of RFamide and *Hym-355* neurons could have various causes: (i) a loss of ISC proliferation necessary to replenish the stock of nerve cells, (ii) a disrupted differentiation of neuronal progenitors or

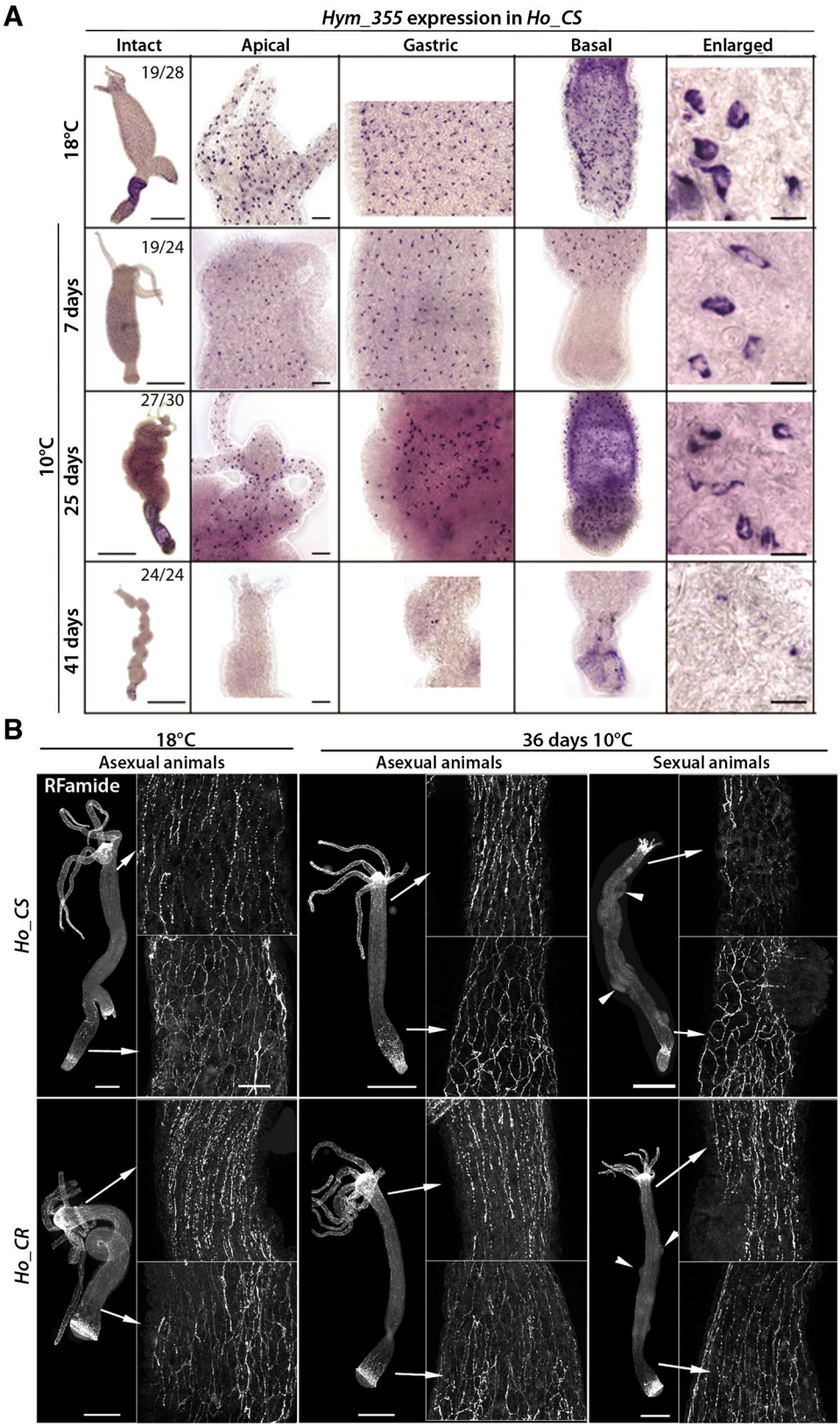
A
Hym_355 expression in *Ho_CS*
Intact
Apical
Gastric
Basal
Enlarged
18°C
19/28
10°C
7 days
19/24
25 days
27/30
41 days
24/24
B
18°C
Asexual animals
36 days 10°C
Asexual animals
Sexual animals
RFamide
Ho_CS
Ho_CR

Figure 4 Loss of neuronal density in *Ho_CS* animals undergoing aging. (A) *Hym-355* expressing nerve cells detected by *in situ* hybridization along the body column of *Ho_CS* animals maintained at 18°C or 10°C for 7, 25, or 41 days. Scale bars: 500 µm (intact), 50 µm (apical, gastric, and basal), 10 µm (enlarged). (B) RFamide expressing nerve cells immunodetected in *Ho_CS* and *Ho_CR* animals maintained at 18°C or 10°C for 36 days. Arrowheads indicate mature or post-mature testes. Scale bars: 100 µm. [Colour figure can be viewed at wileyonlinelibrary.com]

(iii) a poor survival of the newly differentiated neurons. After transfer to 10°C both *Ho_CS* and *Ho_CR* exhibit a decrease in body size due to the change in the feeding rhythm, from four feedings per week at 18°C to two feedings at 10°C. However in *Ho_CS* animals this size decrease strongly affects the head structures that become three fold smaller within 35 days (Fig. 5A). As a consequence of the massive production of gametes, the proliferation of somatic interstitial cells measured after a 24 h BrdU pulse drops to reach a minimal value after 32 days at 10°C, leading to a severe depletion of the stock of somatic ISCs as previously reported (Yoshida *et al*., 2006; Tomczyk *et al*., 2017). However, the rare somatic ISCs that survive readily cycle at later time-points (Fig. 5B).

To visualize the neuronal progenitors in *Ho_CS* animals taken at 44 or 45 days after transfer to cold, we detected the cells expressing *prdl-a* either by *in* situ hybridization (Fig. 5C) or by immunodetection with the antibody raised against *Hydra* prdl-a (Fig. 5D).

At 18°C *prdl-a* is predominantly expressed in neuronal progenitors located in the apical region, a pattern also observed in *Ho_CR* animals maintained at 10°C for 45 days (Fig. 5C). By contrast, *Ho_CS* animals maintained at 10°C for 45 days have very few apical cells expressing *prdl-a*, while some ectopic patches of non-neuronal *prdl-a* cells can be found in the body column. As anticipated, prdl-a protein in *Ho_CR* and *Ho_CS* animals maintained at 18°C is predominantly apical and nuclear (Fig. 5D, arrowheads), a pattern that remains stable in *Ho_CR* maintained at 10°C for 44 days. By contrast, in aging *Ho_CS* we observed a drastic decrease in the number of prdl-a$^+$ cells, likely reflecting a decrease in the number of neuronal precursors. The loss of apical prdl-a$^+$ cells suggests that the deterioration of the nervous system in aging *Ho_CS* is predominantly caused by the lack of *de novo* homeostatic neurogenesis, responsible for the insufficient renewal of the apical nervous system.

Aging-Induced Modulations of Genes Potentially Involved in Neurogenesis and Neurotransmission

To further characterize the changes that occur in the nervous system of aging *Hydra,* we analyzed by quantitative RNA-seq (qRNA-seq) the expression of genes potentially associated with neurogenesis (195) and neurotransmission (377), as previously annotated by Wenger *et al.* (2016). We retrieved the expression levels of these genes in *Ho_CS* and *Ho_CR* animals maintained at 10°C for 14, 26, 32, 35, and 45 days (only *Ho_CS*) as previously reported (Tomczyk *et al*., 2017). Concerning the three *RFamide* genes (Hansen *et al*., 2000), *RFamide A* and *RFamide B* show very similar profiles in the two strains except an upregulation of *RFamideA* in *Ho_CS* at 45 days (Fig. 6A). The persistence of the *RFamideA* transcripts in *Ho_CS* can be linked to their presumptive upregulation in the persisting neurons and/or to their ectopic expression in non-neuronal cell types. *RFamide C*, which is no longer expressed after 25 days at 10°C in *Ho_CR*, exhibits a burst of expression at day-25 in *Ho_CS* to become undetectable at day-45. Concerning *prdl-a,* we found its expression seemingly identical between *Ho_CS* and *Ho_CR* animals, a result compatible with the patterns detected by *in situ* hybridization (Fig. 6A).

To get more global view of the modulations affecting the neurogenesis and neurotransmission genes, we produced heatmaps comparing gene expression levels in each strain (Fig. 6B–G). Among the 195 genes potentially associated with neurogenesis, we found 67 genes that are differently modulated in *Ho_CS* and *Ho_CR*, with 27 genes upregulated in *Ho_CS* but not in *Ho_CR* (Fig. 6B), and 40 genes upregulated in *Ho_CR* but not in *Ho_CS* (Fig. 6E). The former group that includes *Dlx, Dlx1, ELAV-A, ETS1, Fral2, Gli3, KLF8, Meis1, Otx1, Otx2B-1, PUM2, Sox123,* and *TCF15* (Fig. 6B) might correspond to genes upregulated in the remaining epithelial cells after the loss of the interstitial lineage, and/or to genes linked to the persisting gametogenesis in *Ho_CS*. The second group likely includes genes involved in the wave of *de novo* neurogenesis that follows gametogenesis in *Ho_CR* but not in *Ho_CS* (Fig. 6C). Among these 40 genes upregulated in *Ho_CR*, one finds genes associated with interstitial stemness like *Myc-1, Pax-A, ZNF845*, or *Nanos2* (Mochizuki *et al*., 2000; Hobmayer *et al*., 2012; Wenger *et al*., 2016). Loss of sustained expression of these genes in *Ho_CS* likely corresponds to the definitive loss of ISCs and progenitors. Interestingly *LMX1A*, which is upregulated in epithelial cells of HU-treated animals (Wenger *et al*., 2016) is found in this category, suggesting that ESCs in aging

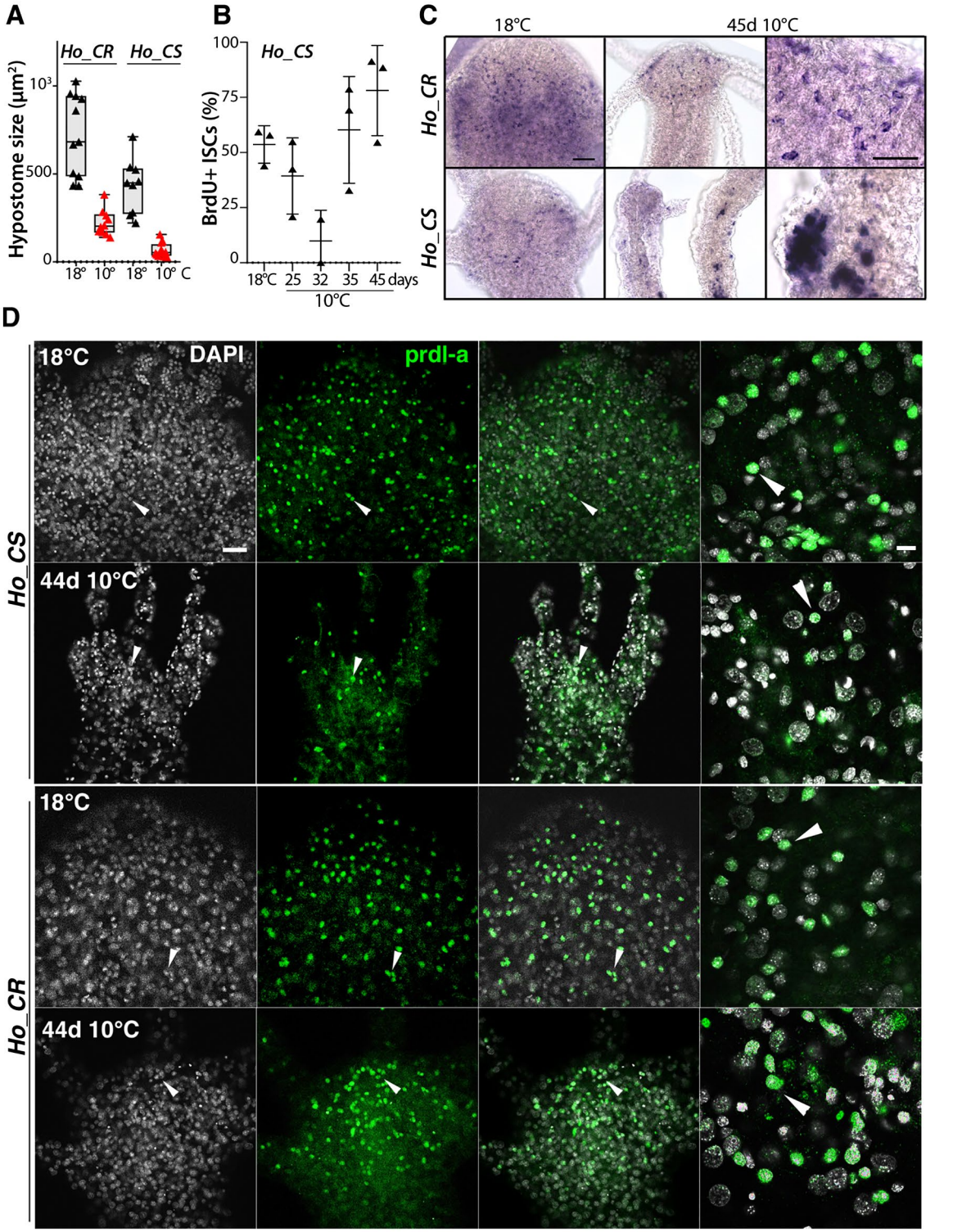

Figure 5 Loss of neuronal progenitors and *prdl-a*/prdl-a expression in aging *H. oligactis*. (A) Decrease in hypostome size in *Ho_CS* and *Ho_CR* animals maintained at 18°C or 10°C for 35 days. (B) Transient decrease in interstitial cycling cells in *Ho_CS*. (C) Apical expression of *prdl-a* in *Ho_CS* and *Ho_CR* animals maintained at 18°C or 10°C for 45 days. (D) Immunodetection of the homeoprotein prdl-a in *Ho_CS* and *Ho_CR* animals maintained at 18°C or taken 44 days after transfer to 10°C. Scale bars: 20 µm (left panels) and 10 µm (right panels). Note the progressive decrease in the number of prdl-a expressing cells in aging *Ho_CS* when compared to *Ho_CR* maintained in the same conditions. [Colour figure can be viewed at wileyonlinelibrary.com]

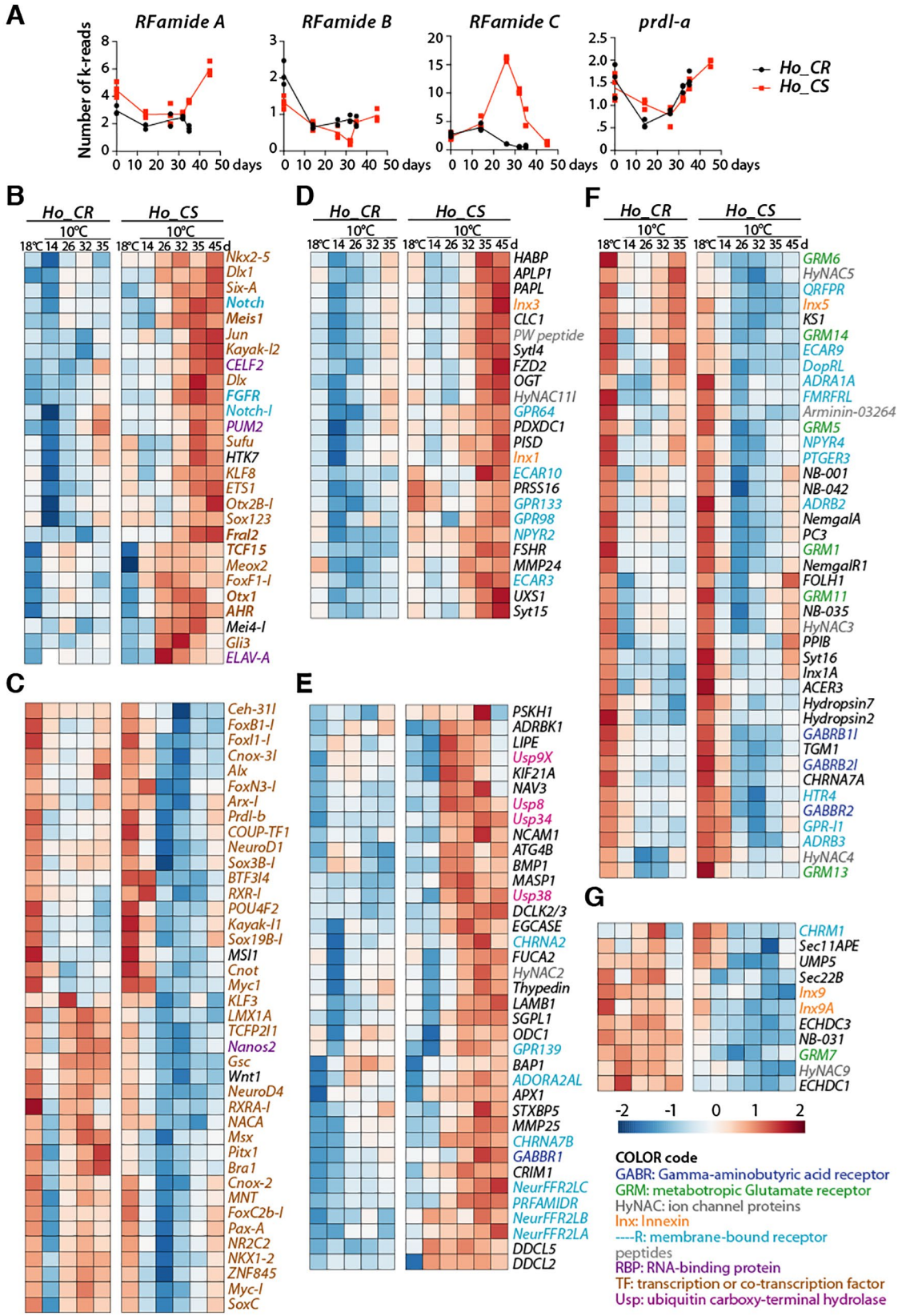
A
RFamide A
RFamide B
RFamide C
prdl-a
Number of k-reads
Ho_CR
Ho_CS
0 10 20 30 40 50 days
B
C
D
E
F
G
Ho_CR
Ho_CS
10°C
18°C 14 26 32 35 45d
Nkx2-5
Dlx1
Six-A
Notch
Meis1
Jun
Kayak-I2
CELF2
Dlx
FGFR
Notch-I
PUM2
Sufu
HTK7
KLF8
ETS1
Otx2B-I
Sox123
Fral2
TCF15
Meox2
FoxF1-I
Otx1
AHR
Mei4-I
Gli3
ELAV-A
Ceh-31I
FoxB1-I
FoxI1-I
Cnox-3I
Alx
FoxN3-I
Arx-I
Prdl-b
COUP-TF1
NeuroD1
Sox3B-I
BTF3I4
RXR-I
POU4F2
Kayak-I1
Sox19B-I
MSI1
Cnot
Myc1
KLF3
LMX1A
TCFP2I1
Nanos2
Gsc
Wnt1
NeuroD4
RXRA-I
NACA
Msx
Pitx1
Bra1
Cnox-2
MNT
FoxC2b-I
Pax-A
NR2C2
NKX1-2
ZNF845
Myc-I
SoxC
HABP
APLP1
PAPL
Inx3
CLC1
PW peptide
Sytl4
FZD2
OGT
HyNAC11I
GPR64
PDXDC1
PISD
Inx1
ECAR10
PRSS16
GPR133
GPR98
NPYR2
FSHR
MMP24
ECAR3
UXS1
Syt15
PSKH1
ADRBK1
LIPE
Usp9X
KIF21A
NAV3
Usp8
Usp34
NCAM1
ATG4B
BMP1
MASP1
Usp38
DCLK2/3
EGCASE
CHRNA2
FUCA2
HyNAC2
Thypedin
LAMB1
SGPL1
ODC1
GPR139
BAP1
ADORA2AL
APX1
STXBP5
MMP25
CHRNA7B
GABBR1
CRIM1
NeurFFR2LC
PRFAMIDR
NeurFFR2LB
NeurFFR2LA
DDCL5
DDCL2
GRM6
HyNAC5
QRFPR
Inx5
KS1
GRM14
ECAR9
DopRL
ADRA1A
FMRFRL
Arminin-03264
GRM5
NPYR4
PTGER3
NB-001
NB-042
ADRB2
NemgaIA
PC3
GRM1
NemgaIR1
FOLH1
GRM11
NB-035
HyNAC3
PPIB
Syt16
Inx1A
ACER3
Hydropsin7
Hydropsin2
GABRB1I
TGM1
GABRB2I
CHRNA7A
HTR4
GABBR2
GPR-I1
ADRB3
HyNAC4
GRM13
CHRM1
Sec11APE
UMP5
Sec22B
Inx9
Inx9A
ECHDC3
NB-031
GRM7
HyNAC9
ECHDC1
-2 -1 0 1 2
COLOR code
GABR: Gamma-aminobutyric acid receptor
GRM: metabotropic Glutamate receptor
HyNAC: ion channel proteins
Inx: Innexin
----R: membrane-bound receptor
peptides
RBP: RNA-binding protein
TF: transcription or co-transcription factor
Usp: ubiquitin carboxy-terminal hydrolase

Figure 6 Modulations of neurogenesis and neurotransmission gene expression in *Ho_CS* and *Ho_CR* animals maintained at 18°C or 10°C. (A) Expression profiles of the genes encoding the *RFamide* neuropeptides and the *prdl-a* homeoprotein measured by qRNA-seq in *Ho_CR* (blue) and *Ho_CS* (red) animals at indicated time points after transfer to 10°C. (B-G) Heatmaps showing the relative expression of 67 genes known or expected to regulate neurogenesis (B, C), and 114 genes whose products are predicted to be involved in neurotransmission (D-G) in *Ho_CR* and *Ho_CS* animals transferred to 10°C at day-0. In panels B, D, E, genes are upregulated in aging *Ho_CS* animals, while in panels C, F, and G, genes are either upregulated in *Ho_CR* or downregulated in *Ho_CS*. Sequences from *Hv* orthologs can be found in Table S1 from Wenger et al. (2016), expression profiles of neurogenesis genes are shown in Supplementary Figure S1. All expression profiles are accessible at www.hydratlas.unige.ch for *Hv* sequences, at http://129.194.56.90/blast/ for *Ho_CS* and *Ho_CR* ones after tblastn with *Hv* sequences. [Colour figure can be viewed at wileyonlinelibrary.com]

Ho_CS are not able to upregulate *LMX1A* in response to the loss of neurogenesis.

Among the 377 genes associated with neurotransmission, we found 114 genes with expression profiles differently modulated in *Ho_CS* and *Ho_CR*. We first identified 24 and 37 genes upregulated at late time points in *Ho_CS* but not in *Ho_CR* where a large number show a transient downregulation at day 14 (Fig. 6D, E). This group contains several genes that encode ubiquitin specific peptidases (Usp), which play important roles in the development and the physiology of bilaterian nervous systems as well as in neurodegenerative diseases (Baptista *et al*., 2012). As an example, Usp8 is implicated in the clearance of protein aggregates (Alexopoulou *et al*., 2016) and might in *Ho_CS* be involved in the response of old persisting neurons to the proteomic stress. Another group contains 41 genes similarly downregulated in response to cold exposure in both *Ho_CS* and *Ho_CR*, possibly not linked to the aging process (Fig. 6F). Finally, 11 genes are maintained at high levels in *Ho_CR* but not in *Ho_CS* (Fig. 6G), likely reflecting the regeneration of a functional nervous system in *Ho_CR* but not in *Ho_CS* animals.

Impact of the Loss of Neurogenesis in HU-Treated *H. vulgaris* and in Aging *Ho_CS*

In *Hydra*, the loss of neurogenesis can easily be achieved with anti-proliferative treatments, such as hydroxyurea (HU) or colchicine. Such treatment in *Ho_CS* animals maintained at 18°C, so in the absence of gametogenesis, also leads to an aging phenotype (Tomczyk *et al*., 2017). This scenario resembles the aging process induced by gametogenesis in *Ho_CS* where the depletion of somatic interstitial progenitors leads to the disorganization of the nervous system. To investigate a possible similarity on the genetic level we compared the transcriptomic data obtained in *Ho_CS* and *Ho_CR* maintained at 10°C (Tomczyk *et al*., 2017) to those obtained in HU-treated *H. vulgaris (Hv_sf1)* (Wenger *et al*., 2016). In each context we retrieved the number of reads for the neurogenesis and neurotransmission associated genes in two conditions, at 18 and 10°C day-35 for *Ho_CS* and *Ho_CR* animals (Fig. 7A), in untreated and HU-treated *Hv_sf1* animals taken seven days after HU exposure (Fig. 7B). We calculated the log2 fold change (FC) for all selected genes (Fig. 7C) and produced a scatterplot representation of the changes in gene expression between *Hv_sf1* post-HU and *Ho_CS* or *Ho_CR* maintained at 10°C.

That way, we identified a series of genes strongly upregulated in *Ho_CS* but not in *Ho_CR*. Among the genes upregulated at least fourfold in *Ho_CS*, we identified *ADORA2A-L, CC2D2A, CHRNA9, DDCL2, EGCase, GPR139, GPR157, NCAM1,* and *STK33* as neurotransmission genes (Fig. 7D) and *AHR, Fral2, FGFR, FoxJ3, Jagged, Meis1, Notch, Otx1,* and *TCF15* as neurogenesis genes (Fig. 7E,F). These putative neurogenesis genes are upregulated at least twofold in 35 days old *Ho_CS* animals (blue numbers), much higher than in *Ho_CR* maintained at 10°C for 35 days (black numbers) where their expression is stable or mildly upregulated (*Otx1*, *FGFR*) except in case of *TCF15* that is upregulated 2.5 fold. Their upregulation in *Ho_CS* also contrasts with the stable expression noted in *Hv_sf1* having lost their ISCs upon HU treatment (red numbers) except *Fral2* that is downregulated.

Expression of two genes *Fral2* and *TCF15* was verified by *in situ* hybridization (Fig. 7G). In *Hv*_AEP maintained at RT, both genes are predominantly expressed in cells from the epidermal layer, epithelial cells but also neurons sticking to these cells (Supplemental Figure S1). Consistently, in *Ho_CS* animals maintained at 18°C, we found *Fral2* expressed at high levels in neurons of the apical region and along the body column, and at low levels in epithelial cells, but we did not detect *Fral2*-expressing cells in *Ho_CR* polyps. After 35 days at 10°C, the testes are already post-mature in *Ho_CR* where few *Fral2* expressing

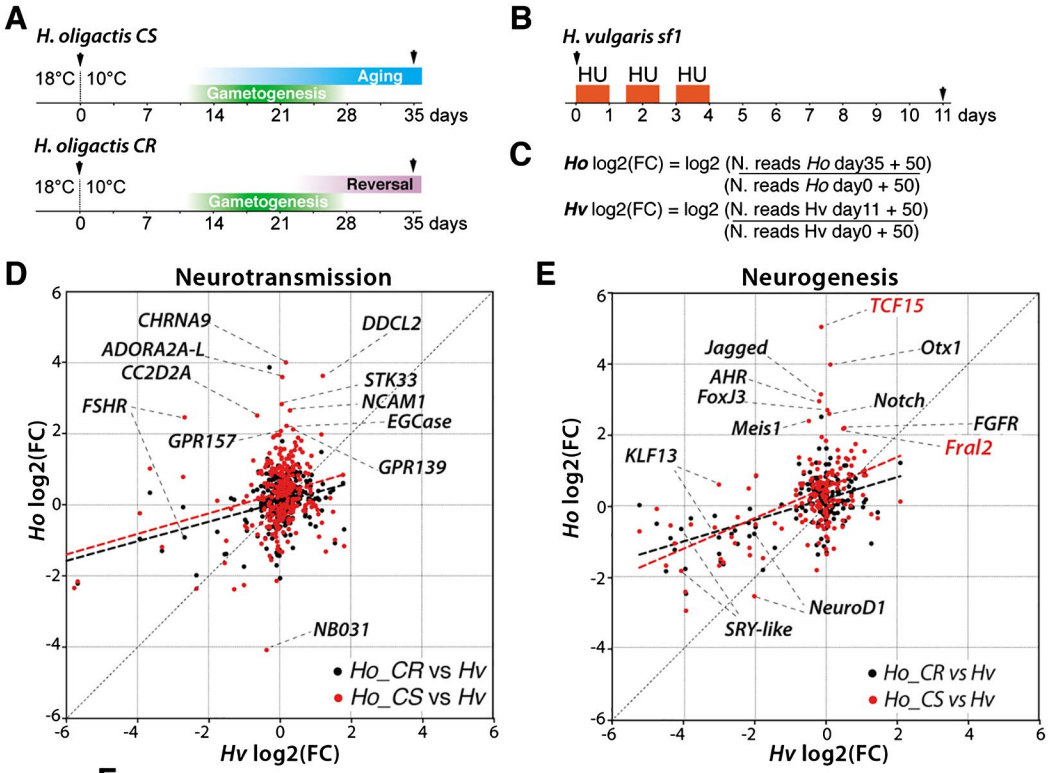

F

Gene name	FC upon interstitial cell loss Ho_CS	Ho_CR	Hv	Protein function	Cell-type expression in asexual animals	Sequence ANs (Hv, Ho, Uniprot/NCBI)
TCF15	5.05	2.51	-0.14	TF	eESCs, ISC derivatives	seq03754; c3558_g1_i01; R023639c0g1; **T2MDV3**
Otx1	3.99	1.35	0.12	TF	**gESC** >> ISC	seq62395; c22001_g2_i02; R028689c0g1; **T2MGP3**
Jagged	3.15	-0.14	-0.15	LIG	ISC > eESC > gESC	seq27299; c12917_g2_i02; R031684c0g1; **G5CCW1**
AHR	2.95	1.62	-0.20	R	**eESC** > gESC, ISC	seq36687; c23901_g2_i01; R034882c0g1; **T2MGK2**
FoxJ3	2.70	0.60	0.03	TF	eESC > ISC > gESC	seq12624; c8168_g1_i01; R034586c0g1; **T2M3A8**
Notch	2.60	0.68	0.09	R	gESC > eESC >> ISC	seq36083; c24101_g1_i02; R034694c0g1; **A8DCL8**
Meis1	2.40	0.46	-0.49	TF	gESC > eESC	seq48362; c17959_g2_i01; R036242c1g3; **T2MJT1**
FGFR	2.20	1.14	0.51	R	eESC > gESC > ISC	seq57558; c25891_g1_i02; R033445c0g1; **Q86PM4**
Fral2	2.18	-0.07	-2.67	TF	neurons (eESCs)	seq74419; c15302_g2_i01; R038935c1g1; **XP_012561111**

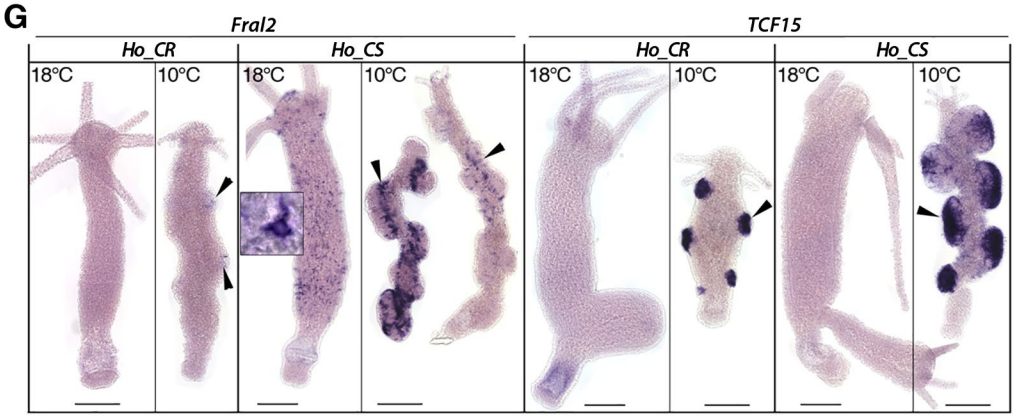

Figure 7 Comparative analysis of gene modulations of neurotransmission and neurogenesis genes in nerve free *H. vulgaris*, *Ho_CS*, and *Ho_CR*. (A, B) Schemes representing the experimental conditions to produce qRNA-seq data (black arrowheads) from *Ho_CS* and *Ho_CR* animals maintained at 10°C for 35 days, or from *Hv_sf1* animals exposed to hydroxyurea (HU). (C) Equations used to calculate the log2 fold change (FC) for *Ho_CS, Ho_CR* animals between day-0 and day-35 of cold exposure, and *Hv_sf1* animals between day-0 and day-11 after HU exposure. (D, E) Scatterplot of FC values from *Hv_sf1* (*x* axis) and *Ho_CS* or *Ho_CR* (*y* axis). The thick dashed lines represent linear regression for the *Ho_CS* (red) and *Ho_CR* (black) conditions. (F) Modulations in the expression of nine neurogenic candidate genes in *Ho_CS* and *Ho_CR* animals maintained at 10°C for 35 days (blue and black numbers, respectively) and in HU-treated *H. vulgaris* (red numbers) as identified in (E). Fold change values (FC) measured in *Ho_CS* and *Ho_CR* animals maintained at 10°C for 35 days or in HU-treated *Hv_sf1* animals were normalized over the values measured in *Ho* animals maintained at 18°C or in untreated *Hv* animals, respectively. LIG: ligand; R: receptor, TF: transcription factor. Detailed expression profiles are shown in Supplementary Figure S1. (G) Expression patterns of *Fral2* and *TCF15* in *Ho_CS* and *Ho_CR* animals maintained at 18°C or at 10°C for 35 days. Scale bar: 200 µm. [Colour figure can be viewed at wileyonlinelibrary.com]

cells can be detected (arrowheads). In aging *Ho_CS* where testes are still fully mature, we found *Fral2* predominantly expressed at the base, where spermatogonia are found. *Fral2* transcripts were also detected in some small cells spread along the body column. This result suggests a role for *Fral2* in spermatogenesis as identified in mice (Cohen *et al*., 1994). Concerning *TCF15* expression, it was undetectable in animals maintained at 18°C, but strong in whole testes (Fig. 7G). These modulations of expression patterns indicate that both genes are upregulated upon gametogenesis, *Fral2* expression being seemingly shifted from the neuronal lineage to the germ cells in testes.

DISCUSSION

In *Hydra* neurogenesis is constantly active although at a low rate in intact adult animals, replacing the neurons that get sloughed off at the extremities throughout the animal life. After bisection, neurogenesis becomes activated and rapidly re-establishes the apical or basal nervous system in the regenerated structure. In this study, we show that the active behaviors are impaired shortly after aging is induced in *Ho_CS* animals. Indeed, contractility or prey capture behaviors become altered long before the loss of nerve cells or the anatomical disorganization of the nervous system are observed. These alterations, behavioral, anatomical, and cellular, are well supported by the molecular analyses. The transcriptomics analysis detects changes in the expression profile of a number of neurotransmission related genes already two weeks after transfer to cold, such as several GABA and glutamate receptors that are downregulated in both *Ho_CS* and *Ho_CR* animals maintained at 10°C. A recent study claims that the neural circuits that mediate the response to glutathione are located in the hypostome and make use of GABA as neurotransmitter (Lauro and Kass-Simon, 2018). As the downregulation of the GABA receptor genes is more pronounced in *Ho_CS* than in *Ho_CR*, this difference might explain the lowered ability of *Ho_CS* to capture preys.

The homeoprotein Prdl-a was initially identified as a marker of apical neuronal progenitors with the expected nuclear localization (Gauchat *et al*., 1998). In aging *Hydra,* that is, sexual *Ho_CS,* but not in *Ho_CR,* we noticed a striking decrease in the number of prdl-a$^+$ cells while the level of *prdl-a* transcripts remained similar between the two strains. After induction of gametogenesis, the number of ISCs rapidly drops in both *Ho_CS* and *Ho_CR* (Yoshida *et al*., 2006; Tomczyk *et al*., 2017), but goes back to the homeostatic level in *Ho_CR* while remaining low in *Ho_CS*. The persistence of prdl-a$^+$ cells in asexual *Ho_CS* and *Ho_CR* animals maintained at 10°C for 44 days suggest that their loss is connected with the aging process. The *prdl-a* RNA-seq expression profile reflects this transient loss of ISCs and the subsequent recovery in *Ho_CR*. In *Ho_CS* the *prdl-a* RNA-seq expression profile is similar but the ISCs population remains depleted suggesting an ectopic, possibly epithelial, upregulation of *prdl-a,* although not detected at the protein level. Indeed, we were able to detect such ectopic expression in patches of *prdl-a* + cells along the body column of aging *Ho_CS*. This ectopic upregulation might be interpreted as an attempt to reactivate neurogenesis in response to the low number of ISCs and neuronal progenitors, but as the epithelial context is not appropriate, the prdl-a protein would not be properly translated or stabilized.

Similarly, the comparative transcriptomic analysis between *Ho_CR* and *Ho_CS* undergoing gametogenesis reflects the intensity of the loss of neurogenesis on the one hand, and the attempt of the aging animals

to rescue neurogenesis on the other hand. Indeed, the loss of mature neurons is well visible in *Ho_CS* but not in *Ho_CR* where the number of neuronal progenitors appears unchanged, implying that in *Ho_CR*, *de novo* neurogenesis is maintained at low pace to replace the old neurons. This state is reflected in the global qRNA-seq results with the heatmaps indicating that large sets of neurotransmission and neurogenesis genes are differently downregulated in *Ho_CR* and *Ho_CS*, mildly and transiently in *Ho_CR,* in a sustained fashion in *Ho_CS*. By contrast, a subset of neurotransmission and neurogenesis genes show the opposite behavior: strongly upregulated in *Ho_CS* while rather downregulated in *Ho_CR*. This second behavior suggests two distinct interpretations: (i) an attempt to rescue neurogenesis in *Ho_CS* by upregulating a series of key genes for neurogenesis; (ii) the capture of neurogenic genes to the benefice of gametogenesis as shown for *Fral2*.

Among these neurogenesis genes *Otx1*, *Otx2*, or *Gli3* are involved in brain development in mammals, while *Dlx1*, *Meis1*, and *PUM2* are involved in neuronal survival and differentiation. *Hydra* interstitial cells are able to sense their density and respond to a lower density by increasing their proliferation rate (David *et al*., 1991). As the number of ISCs and neuronal progenitors strongly decreases in aging *Ho_CS* over the first month, the remaining cells may respond to this low density by over-expressing genes involved in stem cell proliferation and nerve cell differentiation to re-establish the nervous system. This scenario could explain how a large set of genes exhibit similar expression levels between *Ho_CS* and *Ho_CR* despite a dramatically different number of ISCs recorded in these animals when maintained for 35 days at 10°C.

Here, we should mention that the loss of ISCs and interstitial cells is actually more massive and definitive after three courses of HU treatment than in *Ho* animals undergoing gametogenesis (Tomczyk *et al*., 2017; Buzgariu *et al*., 2018). In fact, in HU-treated *Hv-sf1* the depletion of ISCs and neuronal progenitors is almost complete and leads to the complete loss of expression of numerous neurogenic genes (Wenger *et al*., 2016). When we compare the molecular consequences of these two types of neurogenesis loss, we identify nine genes upregulated in aging *Ho_CS* but not at all or to a lower level in the non-aging *Ho_CR*, and at least four-fold in aging *Ho_CS* when compared to HU-treated *Hv_sf1*. For this latter comparison, the results are only indicative as the *Hv* and *Ho* transcriptomes were not generated and processed together, therefore the quantitative approach taken here needs to be confirmed.

Among these genes, we find interestingly *FoxJ3*, initially identified in the neurectoderm of mouse embryos (Landgren and Carlsson, 2004), but also identified as a regulator of spermatogenesis in adult mice (Ni *et al.*, 2016). These genes are either ubiquitously expressed or predominantly expressed in ESCs, suggesting that their upregulation in aging animals takes place either in epithelial cells or in testes as observed here for *Fral2* and *TCF15* by *in situ* hybridization, an experiment that validates the transcriptomic comparative analysis.

Fra-1 and *Fra-2* are bZIP transcription factors initially identified as stress factors that belong to the Fos-related family (Franza *et al.*, 1988). In mammals, they are essential for development, involved in tumorigenesis of multiple organs and in fibrotic diseases (Eferl and Wagner, 2003; Wernig *et al.*, 2017), with a key regulation by the ERK pathway (Gillies *et al.*, 2017). In *Hydra* where five copies of Fra-like genes are found (Supplementary Figure S2), *Fral2* expression switches between asexual and sexual animals, from neurons to male germ cells. As the base of testes contains early spermatogonia that actively proliferate to produce sperm cells, this change in *Fral2* expression suggests a recruitment by the germ cells at the expenses of the nerve cells, a competition process possibly leading to aging. *Fral2* could potentially play a cytoprotective function in this highly active cell population. The low epidermal expression of *TCF15* in standard asexual conditions versus the high gonadic expression in aging animals suggests that in sexual *Hydra TCF15* is recruited to play a role in gametogenesis. In mammals TCF15 is a transcription factor implicated in the priming of the pluripotent embryonic stem cells toward differentiation (Davies *et al.*, 2013).

In summary, we demonstrate an aging-dependent loss of the function, density and organization of nervous system in *Hydra*. These adverse changes are caused by a partial loss of ISCs and neuronal progenitors that occurs as a consequence of the intense production of gametes from ISCs. We identify some candidate regulators of this somatic to germinal switch as *Fral2*, pointing to a possible competition for molecular resources between the somatic – neuronal- and germ cell fate of ISCs.

The authors thank C. Grimmelikhuijzen (Copenhagen) for kindly providing the anti-RFamide antibody, Y. Wenger for the assistance with the transcriptomic analyses.

LITERATURE CITED

Alexopoulou, Z., Lang, J., Perrett, R.M., Elschami, M., Hurry, M.E.D., Kim, H.T., *et al.* (2016) Deubiquitinase

Usp8 regulates α-synuclein clearance and modifies its toxicity in Lewy body disease. *Proceedings of the National Academy of Sciences of the United States of America*, 113, E4688–E4697.

Anderson, P.A. and Spencer, A.N. (1989) The importance of cnidarian synapses for neurobiology. *Journal of Neurobiology*, 20, 435–457.

Baptista, M.S., Duarte, C.B. and Maciel, P. (2012) Role of the ubiquitin-proteasome system in nervous system function and disease: using *C. elegans* as a dissecting tool. *Cellular and Molecular Life Sciences*, 69, 2691–2715.

Bode, H.R., Berking, S., David, C., Gierer, A., Schaller, H. and Trenker, E. (1973) Quantitative analysis of cell types during growth and regeneration in hydra. *Roux's Archives of Developmental Biology*, 171, 269–285.

Bode, H., Lengfeld, T., Hobmayer, B. and Holstein, T.W. (2008) Detection of expression patterns in Hydra pattern formation. *Methods in Molecular Biology*, 469, 69–84.

Boya, P., Codogno, P. and Rodriguez-Muela, N. (2018) Autophagy in stem cells: repair, remodelling and metabolic reprogramming. *Development*, 145, dev146506.

Brien, P. (1953) La pérennité somatique. *Biological Reviews*, 28, 308–349.

Buzgariu, W., Al Haddad, S., Tomczyk, S., Wenger, Y. and Galliot, B. (2015) Multi-functionality and plasticity characterize epithelial cells in Hydra. *Tissue Barriers*, 3, e1068908.

Buzgariu, W., Wenger, Y., Tcaciuc, N., Catunda-Lemos, A.P. and Galliot, B. (2018) Impact of cycling cells and cell cycle regulation on Hydra regeneration. *Developmental Biology*, 433, 240–253.

Campbell, R.D. (1976) Elimination by Hydra interstitial and nerve cells by means of colchicine. *Journal of Cell Science*, 21, 1–13.

Cohen, D.R., Sinclair, A.H. and McGovern, J.D. (1994) SRY protein enhances transcription of Fos-related antigen 1 promoter constructs. *Proceedings of the National Academy of Sciences of the United States of America*, 91, 4372–4376.

Collins, A.G., Schuchert, P., Marques, A.C., Jankowski, T., Medina, M. and Schierwater, B. (2006) Medusozoan phylogeny and character evolution clarified by new large and small subunit rDNA data and an assessment of the utility of phylogenetic mixture models. *Systematic Biology*, 55, 97–115.

David, C.N. (1973) A quantitative method for maceration of hydra tissue. *Roux's Archives of Developmental Biology*, 171, 259–268.

David, C.N., Fujisawa, T. and Bosch, T.C.G. (1991) Interstitial stem cell proliferation in hydra: evidence for strain-specific regulatory signals. *Developmental Biology*, 148, 501–507.

Davies, O.R., Lin, C.Y., Radzisheuskaya, A., Zhou, X., Taube, J., Blin, G., *et al.* (2013) Tcf15 primes pluripotent cells for differentiation. *Cell Reports*, 3, 472–484.

Eferl, R. and Wagner, E.F. (2003) AP-1: a double-edged sword in tumorigenesis. *Nature Reviews Cancer*, 3, 859–868.

Franza, B.R., Jr., Rauscher, F.J., 3rd., Josephs, S.F. and Curran, T. (1988) The Fos complex and Fos-related antigens recognize sequence elements that contain AP-1 binding sites. *Science*, 239, 1150–1153.

Fujisawa, T. (1989) Role of interstitial cell migration in generating position-dependent patterns of nerve cell differentiation in Hydra. *Developmental Biology*, 133, 77–82.

Galliot, B. and Quiquand, M. (2011) A two-step process in the emergence of neurogenesis. *European Journal of Neuroscience*, 34, 847–862.

Galliot, B., Quiquand, M., Ghila, L., de Rosa, R., Miljkovic-Licina, M. and Chera, S. (2009) Origins of neurogenesis, a cnidarian view. *Developmental Biology*, 332, 2–24.

Gauchat, D., Escriva, H., Miljkovic-Licina, M., Chera, S., Langlois, M.C., Begue, A., *et al.* (2004) The orphan COUP-TF nuclear receptors are markers for neurogenesis from cnidarians to vertebrates. *Developmental Biology*, 275, 104–123.

Gauchat, D., Kreger, S., Holstein, T. and Galliot, B. (1998) prdl-a, a gene marker for hydra apical differentiation related to triploblastic paired-like head-specific genes. *Development*, 125, 1637–1645.

Gillies, T.E., Pargett, M., Minguet, M., Davies, A.E. and Albeck, J.G. (2017) Linear integration of ERK activity predominates over persistence detection in Fra-1 regulation. *Cell Systems*, 5(549–563), e545.

Grens, A., Mason, E., Marsh, J.L. and Bode, H.R. (1995) Evolutionary conservation of a cell fate specification gene: the Hydra achaete-scute homolog has proneural activity in Drosophila. *Development*, 121, 4027–4035.

Grimmelikhuijzen, C.J. (1985) Antisera to the sequence Arg-Phe-amide visualize neuronal centralization in hydroid polyps. *Cell and Tissue Research*, 241, 171–182.

Grimmelikhuijzen, C.J. and Westfall, J.A. (1995a) The nervous systems of cnidarians. *EXS*, 72, 7–24.

Grimmelikhuijzen, C.J.P. and Westfall, J.A. (1995b) The nervous systems of Cnidarians. In: Breidbach, O. and Kutsch, W. (Eds.) The Nervous Systems of Invertebrates: An Evolutionary and Comparative Approach. Basel, Switzerland: Birkhaüser Verlag, pp. 7–24.

Grosvenor, W., Rhoads, D.E. and Kass-Simon, G. (1996) Chemoreceptive control of feeding processes in hydra. *Chemical Senses*, 21, 313–321.

Grunder, S. and Assmann, M. (2015) Peptide-gated ion channels and the simple nervous system of Hydra. *The Journal of Experimental Biology*, 218, 551–561.

Hager, G. and David, C.N. (1997) Pattern of differentiated nerve cells in hydra is determined by precursor migration. *Development*, 124, 569–576.

Hansen, G.N., Williamson, M. and Grimmelikhuijzen, C.J. (2000) Two-color double-labeling in situ hybridization of whole-mount Hydra using RNA probes for five different Hydra neuropeptide preprohormones: evidence for colocalization. *Cell and Tissue Research*, 301, 245–253.

Hobmayer, B., Jenewein, M., Eder, D., Eder, M.K., Glasauer, S., Gufler, S., *et al.* (2012) Stemness in Hydra – a current

perspective. *The International Journal of Developmental Biology*, 56, 509–517.

Lenhoff, H.M. and Lenhoff, S.G. (1988) Trembley's polyps. *Scientific American*, 108–113.

Kass-Simon, G. and Pierobon, P. (2007) Cnidarian chemical neurotransmission, an updated overview. *Comparative Biochemistry and Physiology Part A*, 146, 9–25.

Koizumi, O. (2007) Nerve ring of the hypostome in hydra: is it an origin of the central nervous system of bilaterian animals? *Brain, Behavior and Evolution*, 69, 151–159.

Landgren, H. and Carlsson, P. (2004) FoxJ3, a novel mammalian forkhead gene expressed in neuroectoderm, neural crest, and myotome. *Developmental Dynamics*, 231, 396–401.

Lauro, B.M. and Kass-Simon, G. (2018) Hydra's feeding response: effect of GABAB ligands on GSH-induced electrical activity in the hypostome of H. vulgaris. *Comparative Biochemistry and Physiology Part A: Molecular & Integrative Physiology*, 225, 83–93.

Loomis, W.F. (1955) Glutathione control of the specific feeding reactions of hydra. *Annals of the New York Academy of Sciences*, 62, 209–228.

Marcum, B.A. and Campbell, R.D. (1978) Development of Hydra lacking nerve and interstitial cells. *Journal of Cell Science*, 29, 17–33.

Marcum, B.A., Fujisawa, T. and Sugiyama, T. (1980) A mutant hydra strain (sf-1) containing temperature-sensitive interstitial cells. In: Tardent, P. and Tardent, R. (Eds.) Developmental and Cellular Biology of Coelenterates. Amsterdam: Elsevier/North Holland, pp. 429–434.

Marlow, H.Q., Srivastava, M., Matus, D.Q., Rokhsar, D. and Martindale, M.Q. (2009) Anatomy and development of the nervous system of Nematostella vectensis, an anthozoan cnidarian. *Developmental Neurobiology*, 69, 235–254.

Martínez, D.E. (1998) Mortality patterns suggest lack of senescence in hydra. *Experimental Gerontology*, 33, 217–225.

Miljkovic-Licina, M., Chera, S., Ghila, L. and Galliot, B. (2007) Head regeneration in wild-type hydra requires de novo neurogenesis. *Development*, 134, 1191–1201.

Miljkovic-Licina, M., Gauchat, D. and Galliot, B. (2004) Neuronal evolution: analysis of regulatory genes in a first-evolved nervous system, the hydra nervous system. *Biosystems*, 76, 75–87.

Mochizuki, K., Sano, H., Kobayashi, S., Nishimiya-Fujisawa, C. and Fujisawa, T. (2000) Expression and evolutionary conservation of nanos-related genes in Hydra. *Development Genes and Evolution*, 210, 591–602.

Ni, L., Xie, H. and Tan, L. (2016) Multiple roles of FOXJ3 in spermatogenesis: a lesson from Foxj3 conditional knockout mouse models. *Molecular Reproduction and Development*, 83, 1060–1069.

Pierobon, P. (2015) Regional modulation of the response to glutathione in Hydra vulgaris. *The Journal of Experimental Biology*, 218, 2226–2232.

Sacks, P.G. and Davis, L.E. (1979) Production of nerveless Hydra attenuata by hydroxyurea treatments. *Journal of Cell Science*, 37, 189–203.

Schaible, R., Scheuerlein, A., Dańko, M.J., Gampe, J., Martínez, D.E. and Vaupel, J.W. (2015) Constant mortality and fertility over age in Hydra. *Proceedings of the National Academy of Sciences of the United States of America*, 112, 15701–15706. 201521002.

Takahashi, T., Koizumi, O., Ariura, Y., Romanovitch, A., Bosch, T.C., Kobayakawa, Y., *et al.* (2000) A novel neuropeptide, Hym-355, positively regulates neuron differentiation in Hydra. *Development*, 127, 997–1005.

Tardent, P. (1995) The cnidarian cnidocyte, a high-tech cellular weaponry. *BioEssays*, 17, 351–362.

Technau, U. and Holstein, T.W. (1996) Phenotypic maturation of neurons and continuous precursor migration in the formation of the peduncle nerve net in Hydra. *Developmental Biology*, 177, 599–615.

Teragawa, C.K. and Bode, H.R. (1995) Migrating interstitial cells differentiate into neurons in hydra. *Developmental Biology*, 171, 286–293.

Tomczyk, S., Fischer, K., Austad, S. and Galliot, B. (2015) Hydra, a powerful model system for aging studies. *Invertebrate Reproduction and Development*, 59, 11–16.

Tomczyk, S., Schenkelaars, Q., Suknovic, N., Wenger, Y., Ekundayo, K., Buzgariu, W., *et al.* (2017) Deficient autophagy drives aging in Hydra. *bioRxiv*. https://doi.org/10.1101/236638.

Wenger, Y., Buzgariu, W. and Galliot, B. (2016) Loss of neurogenesis in Hydra leads to compensatory regulation of neurogenic and neurotransmission genes in epithelial cells. *Philosophical Transactions of the Royal Society B: Biological Sciences*, 371, 20150040.

Wernig, G., Chen, S.Y., Cui, L., Van Neste, C., Tsai, J.M., Kambham, N., *et al.* (2017) Unifying mechanism for different fibrotic diseases. *Proceedings of the National Academy of Sciences of the United States of America*, 114, 4757–4762.

Xi, Y., Dhaliwal, J.S., Ceizar, M., Vaculik, M., Kumar, K.L. and Lagace, D.C. (2016) Knockout of Atg5 delays the maturation and reduces the survival of adult-generated neurons in the hippocampus. *Cell Death & Disease*, 7, e2127–e2127.

Yoshida, K., Fujisawa, T., Hwang, J.S., Ikeo, K. and Gojobori, T. (2006) Degeneration after sexual differentiation in hydra and its relevance to the evolution of aging. *Gene*, 385, 64–70.